This paper is a non-peer reviewed preprint submitted to EarthArXiv

Mars' Lowest and Highest Points Revisited

Jim Singh[1]

Abstract

We present revised values for Mars' extreme elevations using a blended digital elevation model (DEM) that combines altimetry collected from the Mars Orbiter Laser Altimeter (MOLA) on NASA's *Mars Global Surveyor* with stereo imagery from the High Resolution Stereo Camera (HRSC) on ESA's *Mars Express*. The widely cited minimum elevation is derived from an earlier MOLA-only DEM which lacks direct altimetry in the region of the true minimum, where interpolation omitted a pit. Using the blended DEM, we identify and measure this feature to produce a revised estimate of Mars' lowest point. The same dataset also enables a reassessment of the position and elevation of the planet's highest point on Olympus Mons.

1. Introduction

Determining the extreme topographic limits of Mars helps to inform our understanding the planet's global morphology, but depends on the accuracy and resolution of the DEMs used. Previous determinations rely primarily on the MOLA DEM [1], which provides global coverage and high vertical accuracy (up to 1m per point) but coarse horizontal resolution (463m/pixel) and gaps in certain areas. Using a blended MOLA+HRSC DEM [2] compiled at 200m/pixel, which combines MOLA's absolute elevation control with the higher spatial detail of HRSC data, we re-evaluate (1) the global minimum, previously located within Badwater crater, and (2) the global maximum, located on Olympus Mons.

All elevation values in this study are given relative to the Martian reference datum - a spherical surface with a radius of 3396.19 km - unless otherwise noted.

2. Methods

Digital elevation analysis was conducted using the Mars Quickmap interface and its associated DEM layers [4]. The approximate locations of the lowest and highest points were initially identified through

[1] Email: jimmyboysingh@gmail.com

elevation masking and cursor-based inspection of pixel values. These regions were refined using polygon selection, and the corresponding DEM cubes were exported and analyzed as GeoTIFFs using custom Python scripts.

CTX imagery of the key features was obtained as screenshots from the corresponding CTX mosaic layer in Quickmap. The *Context Camera* (CTX; ~6 m/pixel; Malin et al., 2007 [5]) aboard the *Mars Reconnaissance Orbiter* provides the source data for this global mosaic. Topographic transects were drawn with Quickmap's path tool, and elevation profiles generated from CSV data exported along these transects and processed in Python. Three-dimensional terrain visualizations were created from exported GeoTIFFs using additional Python-based rendering scripts. Hyperlinks providing direct access to each identified location within Quickmap are also included for reference.

3. Results

3.1. The Lowest Point on Mars: Badwater Crater

3.1.1. Background

An elevation of approximately -8200m has been consistently cited in the literature as the lowest point on Mars, with reported values differing by only a few metres. Voelker et al. (2017) [6] give -8194m, Bernhardt et al. (2016) [7] report -8204m, and Tanaka et al. (2019) [8] -8200m, all stating that this point occurs in Badwater crater. The USGS (2002) Mars topographic map [9] also labels -8200m as the global minimum elevation. All of these values are based on the MOLA dataset.

3.1.2. DEM Comparison and Revised Measurement

Figure 1 shows a CTX image of Badwater crater. Point B marks the MOLA-derived minimum, while point A marks the minimum identified using the MOLA+HRSC DEM. As evident in the figure, point A lies within a central pit of the crater, but point B is offset from it. Figure 2 presents elevation profiles along the X-X′ transect in Figure 1. The MOLA+HRSC DEM reveals the pit morphology clearly, while the MOLA-only profile 'smooths over' the pit. Table 1 lists the measured elevations: the MOLA+HRSC DEM gives a minimum of -8528m, which is 327m lower than the MOLA-derived minimum. Point locations in Mars Quickmap: https://bit.ly/4oDtQcl

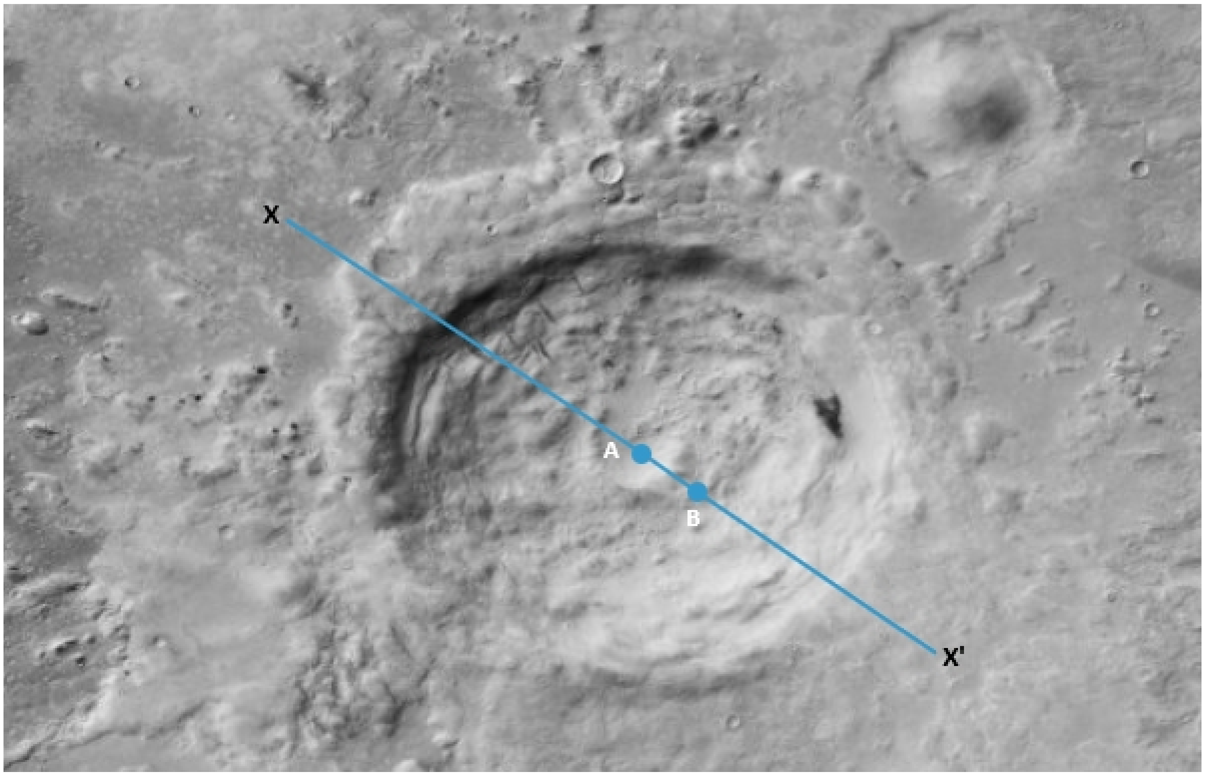

Figure 1: CTX image of Badwater crater

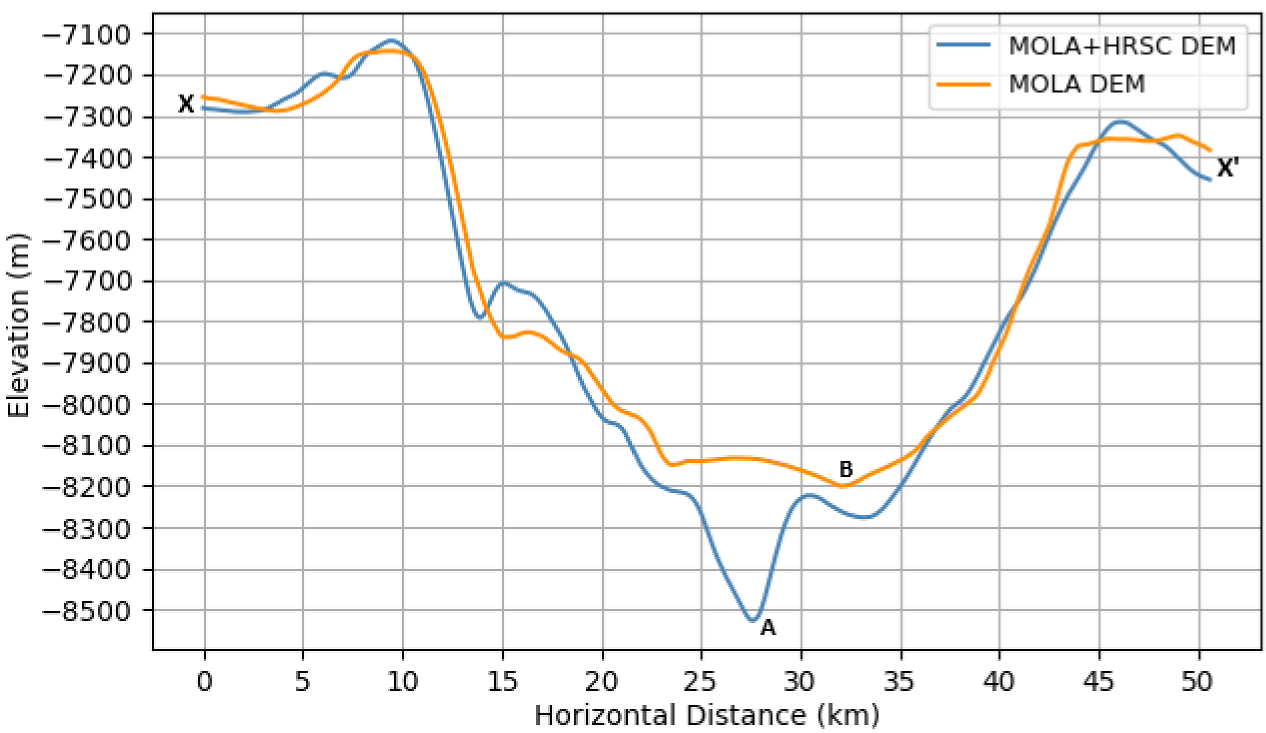

Figure 2: Elevation profiles along the transect shown in Figure 1

DEM	Point	Coordinates [lat, long]	Elevation
MOLA+HRSC	A	[-32.7995°, 62.1403°]	-8528m
MOLA	B	[-32.8475°, 62.2083°]	-8201m

Table 1: Lowest point on Mars with two DEMs

3.1.3. Morphology of the Central Pit

Mars hosts hundreds of central floor pit craters. Badwater is classified as one by Barlow (2010) [10]. Such craters contain a distinct pit near the geometric centre, whose floor lies below the general crater floor level. Barlow (2010) [10] found that most occur within ±40° latitude and that pit-to-crater diameter ratios range from 0.02 to 0.48 (median 0.16). Badwater is 36 km across at its widest, and its central pit is approximately 6 km wide, giving a ratio of 0.17, close to the median value. The average depth of Badwater's pit is 348m, derived from eight terrain profiles drawn radially from the pit's lowest point. For each profile, the elevation difference was measured between the break in slope at the pit wall and the lowest point within the pit; the mean of these eight measurements provides the average pit depth.

3.1.4. Comparison with a Similar Crater

To validate that the measurements obtained for Badwater are representative, a morphometrically similar crater at [-30.8458°, -120.2899°] described by Peel et al., (2019) [11] was examined. It measures 37 km across along the transect in Figure 3 (left panel), with a 7 km pit and a mean pit depth of 358m, determined using the same profiling method. In this case, the pit is distinctly resolved even in the MOLA-only DEM (Figure 3, right panel).

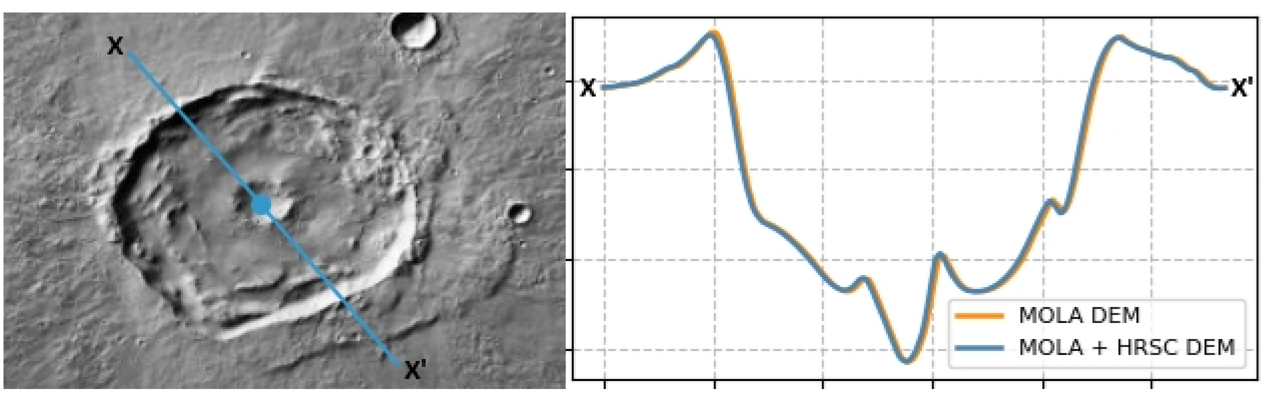

Figure 3: A comparison central floor pit crater

3.1.5. MOLA Data Gaps and the Need for HRSC Integration

Figure 4 compares 3D renders of Badwater crater based on the MOLA DEM (left panel) and MOLA+HRSC DEM (right panel). The MOLA render shows smooth, detail-poor strips across the crater caused by interpolation over missing altimetry tracks, while the blended DEM distinctly resolves the pit, matching CTX imagery in Figure 1.

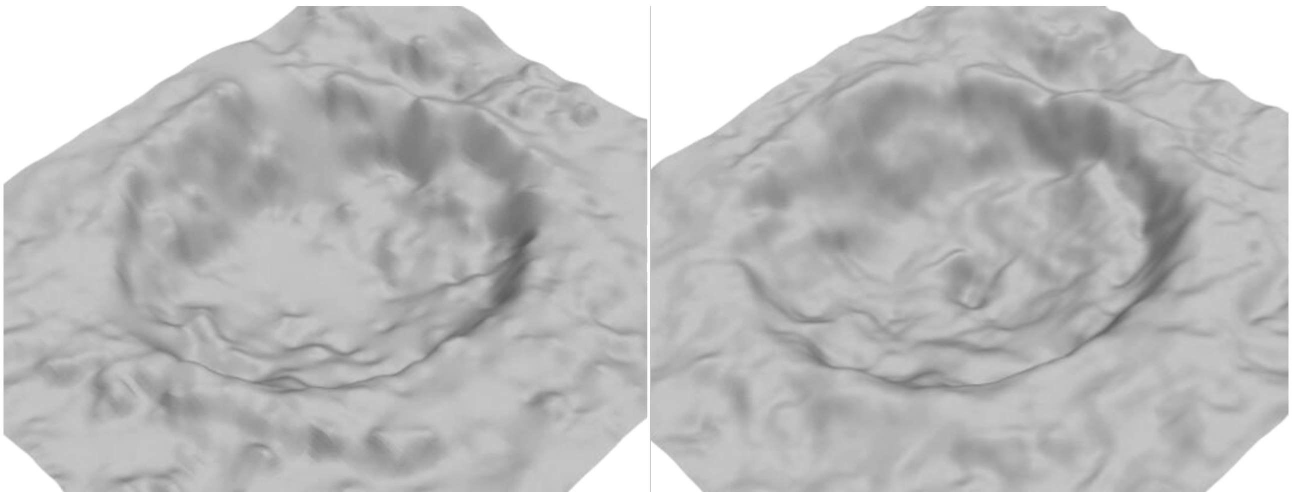

Figure 4: 3D renders of Badwater crater using MOLA DEM (left) and MOLA+HRSC DEM (right)

MOLA data suffers from spatial gaps due to incomplete orbital coverage, intermittent laser firing, and data loss. Interpolation across these gaps can flatten relief, and distort small-scale landforms. (Som et al., 2008) [12]. The HRSC instrument, which reconstructs elevation from multi-angle imagery, provides finer spatial detail (more than 90% surface has been imaged with resolutions up to 10m/pixel; Jaumann et al., 2015 [13]) but requires vertical control. Blending MOLA and HRSC combines the strengths of both datasets - preserving HRSC's morphological fidelity while retaining MOLA's absolute elevation accuracy.

3.2. The Highest Point on Mars: Olympus Mons

3.2.1. Background

The precise elevation and location of Mars' highest point - on Olympus Mons - remain inconsistently reported in the literature. Reported summit elevations vary, mapped positions are not always concordant, and coordinate data are often absent.

For example, Plescia (2004) [14] reported a summit elevation of 21.1 km “above datum” from MOLA data, but gave no location. Mouginis-Mark (2015) [15] presented a CTX-derived DEM profile across Pangboche crater and part of the summit caldera, where the “northern rim crest” of Pangboche appears to reach roughly 21250m relative to “MOLA datum,” inferred from the profile’s vertical scale, though its exact location and significance were not discussed. Later, Mouginis-Mark (2018) [16] placed the highest point at 21205m per “elevation data from MOLA,” south of the summit caldera brink and east of Pangboche, while Mouginis-Mark (2021) [17] reported 21290m, with the caldera “~11 km to the north of this high point.” However, the accompanying map does not show this point, and identifies 21205m as the highest elevation on the volcano, at the same location as Mouginis-Mark (2018) [16], relative to a “mean radius of 3382.9 km.”

3.2.2. Revised Summit Measurement

Figure 5 shows a CTX mosaic of the Olympus Mons summit plateau, including Pangboche crater and the southern edge of the summit caldera (Olympus Paterae). Blue transects cross four key points: the highest on Pangboche’s rim (A), the lowest on its floor (B), and the two highest points on the surrounding plateau (C, D). Point locations in Mars Quickmap: https://bit.ly/4hnEZM3

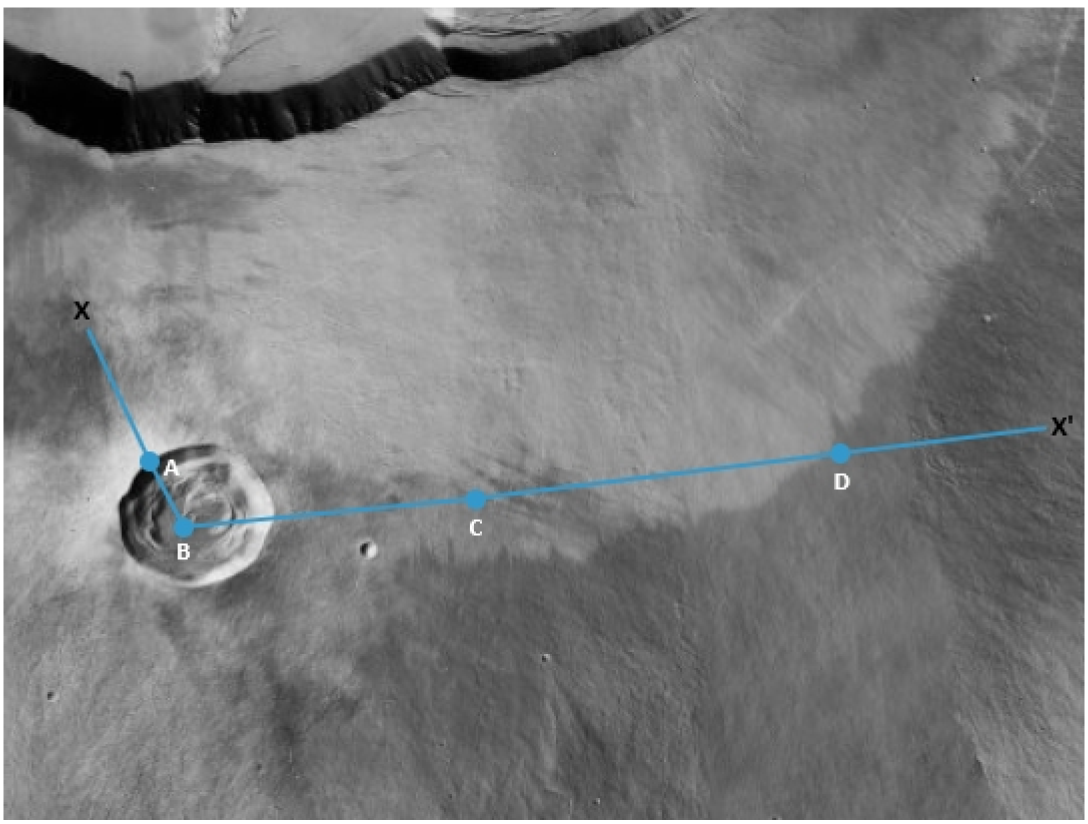

Figure 5: CTX image of Olympus Mons summit, showing Pangboche crater

Figure 6 presents a 3D render of the summit region viewed along the transect from X′, with vertical exaggeration. The brink of Olympus Paterae lies along the right margin of the image. The regional surface slope where Pangboche formed is less than 2°, but the greater height of the crater's upslope rim may have resulted from this tilt (Mouginis-Mark, 2015) [15].

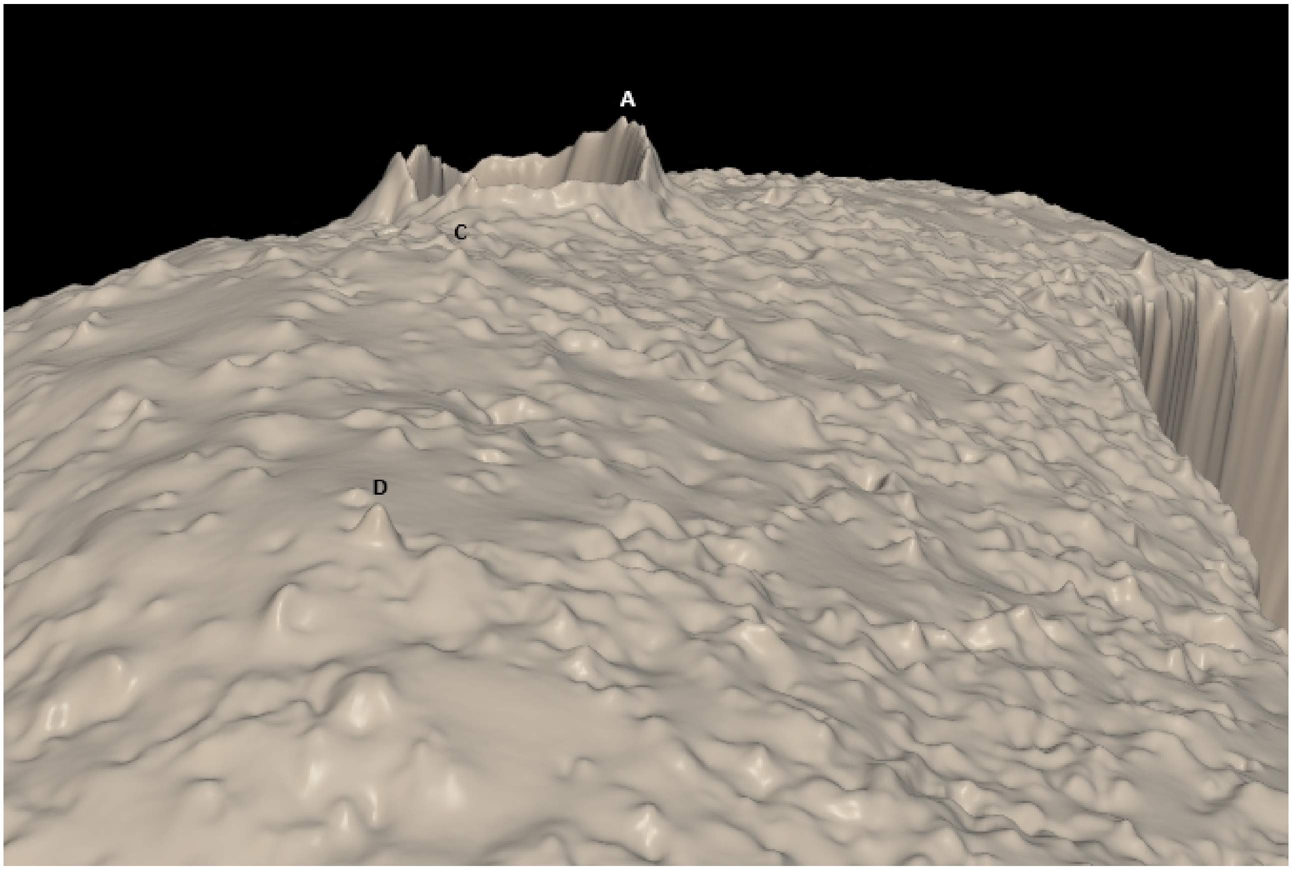

Figure 6: 3D render with MOLA+HRSC DEM of Olympus Mons summit region shown in Figure 5

Figure 7 shows the corresponding elevation profile. The northwestern rim crest of Pangboche (Point A) is identified as the highest point on Mars, at 21226m above datum. The crater's rim rises 276m above the surrounding summit plateau (Table 3).

Points C and D, located 13.5 km and 38.5 km east of Pangboche, are 64m and 63m lower than point A, respectively. The location of point C corresponds to the location (though not the elevation) of the 21205m high point indicated by Mouginis-Mark (2018, 2021) [16][17].

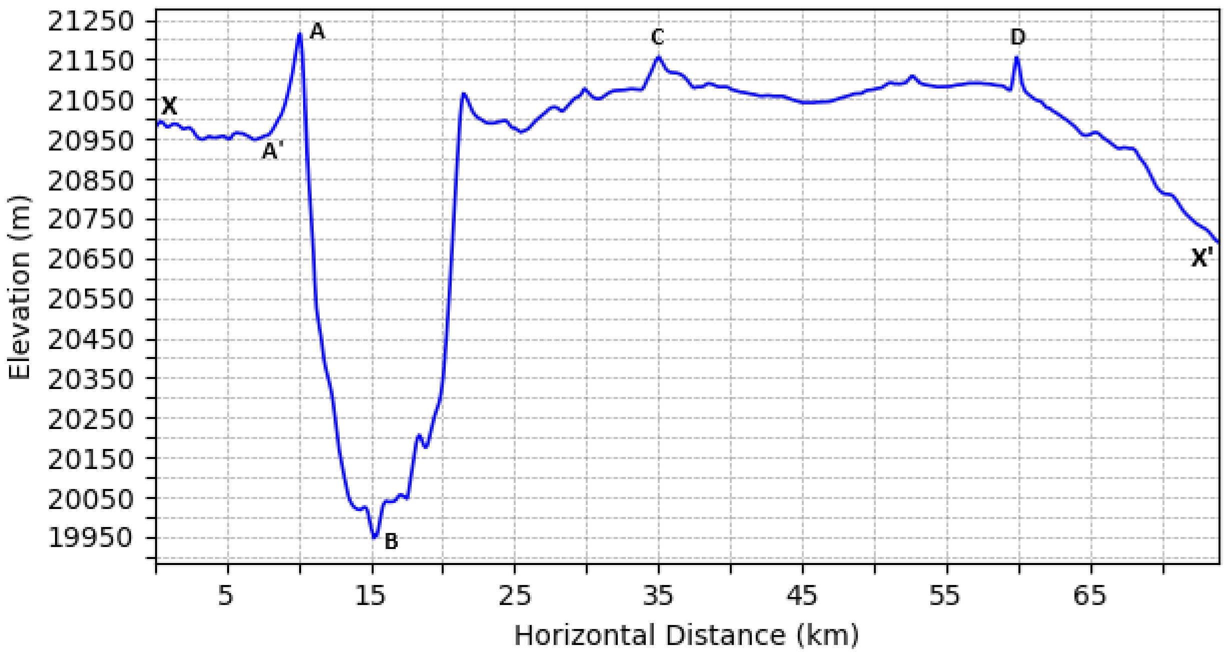

Figure 7: MOLA+HRSC DEM elevation profile along the transect in Figure 5

The measurements derived from the mapped points in Figs 5-7 are presented in Table 2, and relative height differences between points in Table 3.

Point	**Coordinates [lat, long]**	**Elevation**	**Significance**
A	[17.3434°, -133.4489°]	21226m	Rim crest of Pangboche crater. Highest point on Olympus Mons. Highest elevation on Mars.
B	[17.2657°, -133.4084°]	19939m	Lowest point within Pangboche
C	[17.2995°, -133.0609°]	21162m	Highest point 1 on Olympus Mons, excluding Pangboche
D	[17.3534°, -132.6256°]	21163m	Highest point 2 on Olympus Mons, excluding Pangboche

Table 2: Highest point on Olympus Mons, and other notable summit locations

Measure	Value	Significance
A-A’	276m	Maximum rim height of Pangboche: difference in elevation between rim crest, and topographic break in slope with the surrounding terrain
A-B	1287m	Maximum depth of Pangboche: difference in elevation between rim crest, and lowest point in the crater

Table 3: Key elevation differences within Pangboche crater

3.2.3. Geological Context

Pangboche is a roughly polygonal impact crater, 10.8 km at its widest, with a central pit cluster. Its ejecta blanket overlies Olympus Paterae, confirming that it postdates the caldera (Mouginis-Mark, 2021)[17]. Very few impact craters of similar size occur on Olympus Mons, and Pangboche is the only large, fresh impact crater at high elevation on Mars (Mouginis-Mark, 2015) [15]. Its fortuitous placement on the summit plateau means that the planet’s maximum elevation could easily have been at the non-Pangboche high points C and D.

4. Conclusion

This study revises both the lowest and highest elevations on Mars using a blended MOLA+HRSC DEM. The identification of a previously unresolved 6 km pit within Badwater crater lowers the global minimum elevation to -8528m, which is 327m lower than MOLA-based estimates, demonstrating how data gaps in MOLA can obscure local depressions. At the opposite extreme, the maximum elevation of 21226m occurs on the northwestern rim of Pangboche crater on Olympus Mons - several tens of metres higher than anywhere else on the summit plateau - thereby refining previously reported summit values and removing ambiguity about the exact location of Mars’ highest point. These results adjust the known topographic range of Mars to 29.75 km, and highlight the benefit of multi-source elevation models for planetary geomorphology.

5. Acknowledgments

I am grateful to Daniel Quinn and Oscar Argudo for the opportunity to collaborate on a project cataloguing landforms with topographic prominence greater than 1000m on celestial bodies, which provided the foundation for this study. The work follows a 2024 publication documenting 7149 such features on Earth.

I thank Professor Robert Herrick (University of Alaska, Fairbanks) for review of an earlier version of the section on Mars' lowest elevation.

6. References

[1] U.S. Geological Survey Astrogeology Science Center. (2003). *Mars MGS MOLA DEM 463m* [Map]. U.S. Geological Survey Astrogeology Science Center. https://astrogeology.usgs.gov/search/map/mars_mgs_mola_dem_463m

[2] U.S. Geological Survey Astrogeology Science Center. (2018, January 31). *Mars MGS MOLA MEX HRSC blended DEM global 200m* [Map]. U.S. Geological Survey Astrogeology Science Center. https://astrogeology.usgs.gov/search/map/mars_mgs_mola_mex_hrsc_blended_dem_global_200m

[3] Smith, D. E., et al. (2001). Mars Orbiter Laser Altimeter: Experiment summary after the first year of global mapping of Mars. *Journal of Geophysical Research: Planets*, 106(E10), 23689–23722. https://doi.org/10.1029/2000JE001364

[4] Applied Coherent Technology. Mars QuickMap [Interactive map]. https://mars.quickmap.io/

[5] Malin, M. C., et al. (2007), Context Camera Investigation on board the Mars Reconnaissance Orbiter, *J. Geophys. Res.*, 112, E05S04, doi:10.1029/2006JE002808.

[6] Voelker, M., Hauber, E., Schulzeck, F., & Jaumann, R. (2017). Grid-mapping Hellas Planitia, Mars: Insights into distribution, evolution and geomorphology of (peri)-glacial, fluvial and lacustrine landforms in Mars' deepest basin. *Planetary and Space Science*, 145, 49–70. https://doi.org/10.1016/j.pss.2017.07.012

[7] Bernhardt, H., Reiss, D., Hiesinger, H., & Ivanov, M. A. (2016). The honeycomb terrain on the Hellas basin floor, Mars: A case for salt or ice diapirism. *Journal of Geophysical Research: Planets*.

https://doi.org/10.1002/2016JE005007

[8] Tanaka, K. L., Coles, K. S., & Christensen, P. (2019). *The atlas of Mars: Mapping its geography and geology* (pp. 222–227) [Book]. Cambridge University Press. https://doi.org/10.1017/9781139567428.033

[9] U.S. Geological Survey Water Resources Division. (2002). *Topographic map of Mars, M 25M RKN* (Open-File Report 2002-282) [Map]. U.S. Geological Survey. https://doi.org/10.3133/ofr02282

[10] Barlow, N. G. (2010). Central pit craters: Observations from Mars and Ganymede and implications for formation models. *The Geological Society of America Special Paper*, 465.

[11] Peel, S. E., Burr, D. M., & Tran, L. (2019). Formation of central pits in impact craters on Mars: A statistical investigation of proposed mechanisms. *Journal of Geophysical Research: Planets*, 124(2), 314–334. https://doi.org/10.1029/2018JE005738

[12] Som, S. M., Greenberg, H. M., & Montgomery, D. R. (2008). The Mars Orbiter Laser Altimeter dataset: Limitations and improvements. *The International Journal of Mars Science and Exploration*, 3, 2–25. https://doi.org/10.1555/mars.2008.0002

[13] Jaumann, R., Neukum, G., Tirsch, D., Hoffmann, H., & Mars Express HRSC Team. (2015). The High Resolution Stereo Camera (HRSC): Status and facts. *46th Lunar and Planetary Science Conference*. Available at: https://elib.dlr.de/100711/1/1057.pdf

[14] Plescia, J. B. (2004). Morphometric properties of Martian volcanoes. *Journal of Geophysical Research: Planets*, 109(E3). https://doi.org/10.1029/2002JE002031

[15] Mouginis-Mark, P. J. (2015). Cratering on Mars with almost no atmosphere or volatiles: Pangboche crater. *Meteoritics & Planetary Science*, 50(1), 51–62. https://doi.org/10.1111/maps.12400

[16] Mouginis-Mark, P. J. (2018). Olympus Mons volcano, Mars: A photogeologic view and new insights. *Geochemistry*, 78(4), 397–431. https://doi.org/10.1016/j.chemer.2017.11.006

[17] Mouginis-Mark, P. J. (2021). *Geologic map of Olympus Mons caldera, Mars* (Scientific Investigations Map 3470) [Map, scale 1:200,000]. U.S. Geological Survey. https://doi.org/10.3133/sim3470

[18] World Ribus. (n.d.). *Mountains with 1000m of Topographic Prominence*. https://worldribus.org/